Image Processing and the Spline Approximation of the Third and Fifth Order

I.G. Burova, I.I. Narbutovskikh, E.F. Muzafarova

***Abstract* —**Local splines and it's cubic polynomial splines, which are used traditionally, are used in solving many image processing problems. In this paper, we consider the use of local quadratic polynomial and trigonometric splines of the third order of approximation, as well as polynomial splines of the fifth order of approximation for image processing. The paper proposes an algorithm to increase the image (or its part) without loss of quality using local polynomial splines of the third and fifth order of approximation and trigonometric splines of the third order of approximation. This paper also developed an algorithm for compressing and restoring images using the considered splines. The theoretical background and results of numerical experiments are presented.

***Keywords*—** Local polynomial splines, trigonometric splines, image processing

I. Introduction

DIGITAL technologies provide unlimited access to a large amount of diverse information. A significant part of them are problems related to image processing. Currently, many studies are devoted to image processing problems. Automatic face recognition in the wild still suffers from low-quality, low resolution, image noise, and occluded input images that can severely impact identification accuracy.

In paper [1] the authors present a novel technique to enhance the quality of such extreme low-resolution face images beyond the current state of the art. They model the correlation between high and low resolution faces in a multi-resolution pyramid and show that they can recover the original structure of an un-seen extreme low-resolution face image. By exploiting domain knowledge of the structure of the input signal and using sparse recovery optimization algorithms, they can recover a consistent sparse representation of the extreme low-resolution signal. The proposed super-resolution method is robust to noise and face alignment, and can handle extreme low-resolution faces up to 16x magnification factor.

The subtle variations in video may contain some significant information, and the variations may be a tiny motion of objects or ones superimposed on large motion. The state-of-the-art video acceleration magnification method can handle linear large motions while still amplifying small changes. However, it still introduces some artifacts or blurring. In work [2] the authors propose a method to mitigate the issue by adopting a magnification factor adaptive strategy. This strategy is based on analyzing the limitation of magnification factor at different scales of the complex steerable pyramid. In this new approach, magnification factors at various scales are set according to the spatial representative wavelengths of each scale.

Image interpolation plays an important role in converting a low resolution image into a high resolution image. Paper [3] provides a comprehensive study of perdurable image interpolation techniques, such as the cubic spline, and iterative linear interpolation. The usage of a Lagrange polynomial and a piecewise polynomial gives a better fitting curve for interpolated pixel value algorithms.

Image magnification is one of the branches in digital image processing that is often required in various applications, such as in the field of medicine, multimedia, and in satellite imagery. As technology grows, more and more methods are used for image enlargement. In study [4] the image enlargement process is performed by using the Bi-Cubic spline interpolation method. The authors compare the original image with the picture after enlargement.

Inspired by the application of denoising autoencoding priors (DAEP) to image restoration tasks, paper [5] proposes a single image super-resolution (SISR) method via introducing multi-denoising autoencoding priors (MDAEP). On the basis of the naive DAEP, the proposed MDAEP integrates multi-DAEPs from different noisy inputs into the iterative restoration process. The combined strategy avails to alleviate the instability of the denoising autoencoders, and thus to avoid falling into local solutions.

In paper [6] the authors proposed an adaptive remote sensing image magnification approach. An edge stopping function is added to the regularization term of the self-snake model to produce and improve it, which will then have a stronger edge-preservation ability. The adaptive remote sensing image magnification method, which synthesizes the improved self-snake model and Tikhonov regularization by the new weight function, is proposed.

The large volume of medical images remains a major problem for their archiving and transmission. In this context, paper [7] proposes a novel protocol wavREPro that aims to minimize the image size before its storage and then to enlarge it at reception. This process has been achieved by exploiting the Discrete Wavelet Transforms (DWT) namely Haar, Le Gall (5/3) and Daubechies (9/7) wavelets.

I.G.Burova is with the St. Petersburg State University, 7/9 Universitetskaya nab. St. Petersburg, 199034 Russia (i.g.burova@spbu.ru, burovaig@mail.ru)

I.I.Narbutovskikh is with the St. Petersburg State University, 7/9 Universitetskaya nab. St.Petersburg, 199034 Russia (i.narbutovskikh@gmail.com)

E.F. Muzafarova is with the St. Petersburg State University, 7/9 Universitetskaya nab. St. Petersburg, 199034 Russia (e.muzafar@yandex.ru)

The technique of image scaling plays a critical role in the digital image processing applications for the coordination between different display devices. In paper [8] an improved algorithm is proposed by using a controllable sharpness coefficient to obtain better resulting images under different scaling magnifications.

Paper [9] proposes a method, which selects the slices to be projected into a smart synthetic X-ray image in a way which is optimal w.r.t to the sharpness of predefined ROIs (e. g. knee, spine or hip). Therefore, two Laplacian-based auto-focus measures are combined with a thin-plate spline yielding a sharp and homogenous image impression within the smart radiograph. It was shown that the auto-focus method is able to select the same slice as it was selected during an expert annotation. Upon visual inspection, it could be determined that the proposed method achieves higher contrast and clearly better visibility of complex bone structures like spine or hip.

The quantitative assessment of the trabecular bone microarchitecture in the extremity cone-beam CT (CBCT) would benefit from the high spatial resolution, low electronic noise, and fast scan time provided by complementary metal-oxide semiconductor (CMOS) x-ray detectors. Paper [10] is a cascaded systems model of a CMOS x-ray detector incorporating the effects of CsI:Tl scintillator thickness that was developed. The results indicate that the adoption of a CMOS detector in extremity CBCT can benefit applications in quantitative imaging of trabecular microstructure in humans.

Super resolution is the problem of artificially enlarging a low resolution photograph to recover a plausible high resolution version. In the regime of high magnification factors, the problem is dramatically underspecified and many plausible, high resolution images may match a given low resolution image. In work [11] the authors propose a new probabilistic deep network architecture, a pixel recursive super resolution model, that is an extension of PixelCNNs to address this problem.

Paper [12] demonstrates the use of two-coloured digital holographic microscopy (DHM) for imaging microbiological subjects. The use of two wavelengths significantly reduces artifacts present in the reconstructed data, allowing it to image weakly-scattering objects in close proximity to strongly-scattering objects. The authors demonstrate this by reconstructing the shape of the flagellum of a unicellular eukaryotic parasite Leishmania mexicana in close proximity to a more strongly-scattering cell body.

In [13] a sub-pixel disparity refinement algorithm based on the Lagrange interpolation is proposed to calculate the sub-pixel disparity and the elevation of the target construction on the remote sensing image. The accurate integer matching feature points are obtained by an improved affine scale invariant feature transform. A series of interpolation samples can be estimated through the three times magnification results of each feature matching point and its close neighbor pixels. The final sub-pixel deviation can be calculated by the interpolation samples.

The purpose of paper [14] is to investigate the image acquisition parameters in medcine imaging modality.

Paper [15] which deals with image scaling, is the procedure of resizing a digital image. The digital image is converted from low to high resolution and low to high dimension without losing the natural content. It has many phrases in document such as image bilinear interpolation, images resampling, digital resizing, image magnification.

Paper [16] performs a comparative study of the results of some interpolation and resampling techniques for speech and audio signals. The techniques are compared on the basis of quality of reconstruction and computational cost. The authors consider the following interpolation techniques: 1) linear; 2) shifted linear; 3) Keys cubic; and 4) cubic B-spline. These techniques have been extensively applied in image processing applications such as magnification and rotation. The authors study the efficacy of these techniques in resampling speech and audio signals. The authors observe that, in terms of the quality of signal reconstruction, the techniques can be ranked in decreasing order of performance as follows: cubic B-spline, keys cubic, shifted linear, and piecewise-linear interpolation. In terms of computational cost, the interpolation techniques, arranged in ascending order of time taken are as follows: piecewise-linear interpolation, shifted linear, keys cubic, and cubic B-spline. However, they note that the shifted linear interpolation technique gives a significant improvement in quality with just a small increase in computational cost. This might be particularly important in embedded and real-time applications where processing time is critical.

Questions related to the processing of numerical streams associated with compression and recovery are considered in many papers. Visualization of vector fields plays an important role in many applications. Paper [17] describes a new approach for vector field null points detection and evaluation, which enables data compression and easier fundamental behavior visualization.

Adaptive algorithms of spline-wavelet decomposition in a linear space over metrized field are proposed in [18].

This paper is a work from the cycle of work on the topic of applying local integro-differential splines to the processing of flows of numerical information and image processing [19]-[21].

Despite the huge variety of practical processing tasks, they are reduced to a small number of basic tasks, among which should be noted the resizing of the image, including the restoration of missing sections, image compression. Here will be considered possible solutions for image processing and numerical information flows using spline approximations.

II. Polynomial splines

A. Polynomial splines of the third order of approximation

First consider the features of the application of splines of the third order of approximation.

Let a, b be real numbers, $\{t_j\}$ be a set of equidistant nodes on $[a,b]$, $t_j = a + j\,h, j = 0, \dots, n,\ \ h = t_{j+1} - t_j$. Let the function $u \in C^3[a,b]$. We construct the left quadratic polynomial splines solving the system of equations

$$t_j^k w_j(t) + t_{j+1}^k w_{j+1}(t) + t_{j+2}^k w_{j+2}(t) = t^k,$$

$$k = 0, 1, 2, t \in [t_j,\ t_{j+1}].$$

The solution of this system may be written in the form:

$$w_j(t) = \frac{t - t_{j+1}}{t_j - t_{j+1}} \cdot \frac{t - t_{j+2}}{t_j - t_{j+2}},$$
$$w_{j+1}(t) = \frac{t - t_j}{t_{j+1} - t_j} \cdot \frac{t - t_{j+2}}{t_{j+1} - t_{j+2}},$$
$$w_{j+2}(t) = \frac{t - t_j}{t_{j+2} - t_j} \cdot \frac{t - t_{j+1}}{t_{j+2} - t_{j+1}}.$$

Using these splines we construct the approximation in the form:

$$U^L(t) = u_j w_j(t) + u_{j+1} w_{j+1}(t) + u_{j+2} w_{j+2}(t),.$$
$$t \in [t_j,\ t_{j+1}]$$

We construct the right quadratic polynomial splines solving the system of equations

$$t_{j-1}^k w_{j-1}(t) + t_j^k w_j(t) + t_{j+1}^k w_{j+1}(t) = t^k,$$
$$k = 0, 1, 2,\ t \in [t_j,\ t_{j+1}].$$

The solution of this system may be written in the form:

$$w_j(t) = \frac{t - t_{j+1}}{t_j - t_{j+1}} \cdot \frac{t - t_{j-1}}{t_j - t_{j-1}},$$
$$w_{j+1}(t) = \frac{t - t_j}{t_{j+1} - t_j} \cdot \frac{t - t_{j-1}}{t_{j+1} - t_{j-1}},$$
$$w_{j-1}(t) = \frac{t - t_j}{t_{j-1} - t_j} \cdot \frac{t - t_{j+1}}{t_{j-1} - t_{j+1}}.$$

Using these splines we construct the approximation in the form:

$$U^R(t) = u_{j-1} w_{j-1}(t) + u_j w_j(t) + u_{j+1} w_{j+1}(t).$$

Theorem 1. The error of the approximation with the left polynomial splines, of the third order approximation, is the following:

$$\|u - U^L\|_{[t_j, t_{j+1}]} \le K h^3/3!\ \|u^{(3)}\|_{[t_j, t_{j+2}]},$$
$$K = 0.385.$$

The error of the approximation with the right polynomial splines, of the third order approximation, is the following:

$$\|u - U^R\|_{[t_j, t_{j+1}]} \le K h^3/3!\ \|u^{(3)}\|_{[t_{j-1}, t_{j+1}]}$$
$$K = 0.385.$$

Proof. The proof of the theorem is based on the application of the Lagrangian interpolation remainder formula.

Table I shows the factual errors in absolute values of the approximation of function $u(x)$ when we use the left and the right polynomial splines of the third order approximation when $[a, b] = [-1,1], h = 0.1$.

Table I. The factual errors of approximation with the left and the right polynomial splines

Function $\boldsymbol{u(x)}$	The factual error of approximation	
	The Left splines	*The Right splines*
$\frac{1}{1 + 25x^2}$	0.0296	0.0296
$\sin(x)\cos(2x)$	0.000864	0.000864

B. Polynomial splines of the fifth order of approximation

Now, we need the fifth-order spline approximation formulas. We cannot use the middle splines the fifth-order approximation near the boundaries of interval $[a, b]$ but as in two grid intervals. The approximation with the middle splines can be written as follows:

$$V_4^M(t) = \sum_{j=i-2}^{j=i+2} u(t_j) w_j(t),\ t \in [t_i, t_{i+1}],$$

where

$$w_{i-2}(t) = \frac{(t - t_{i-1})(t - t_i)(t - t_{i+1})(t - t_{i+2})}{(t_{i-2} - t_{i-1})(t_{i-2} - t_i)(t_{i-2} - t_{i+1})(t_{i-2} - t_{i+2})},$$
$$w_{i-1}(t) = \frac{(t - t_{i-2})(t - t_i)(t - t_{i+1})(t - t_{i+2})}{(t_{i-1} - t_{i-2})(t_{i-1} - t_i)(t_{i-1} - t_{i+1})(t_{i-1} - t_{i+2})},$$
$$w_i(t) = \frac{(t - t_{i-2})(t - t_{i-1})(t - t_{i+1})(t - t_{i+2})}{(t_i - t_{i-2})(t_i - t_{i-1})(t_i - t_{i+1})(t_i - t_{i+2})},$$
$$w_{i+1}(t) = \frac{(t - t_{i-2})(t - t_{i-1})(t - t_i)(t - t_{i+2})}{(t_{i+1} - t_{i-2})(t_{i+1} - t_{i-1})(t_{i+1} - t_i)(t_{i+1} - t_{i+2})},$$
$$w_{i+2}(t) = \frac{(t - t_{i-2})(t - t_{i-1})(t - t_i)(t - t_{i+1})}{(t_{i+2} - t_{i-2})(t_{i+2} - t_{i-1})(t_{i+2} - t_i)(t_{i+2} - t_{i+1})}.$$

We can use the left splines near the left boundary of the interval $[a, b]$ but not near the right boundary of the interval $[a, b]$ as in four grid intervals. The approximation with the right splines can be written as follows:

$$V_4^L(t) = \sum_{j=i}^{j=i+4} u(t_j) w_j(t),\ t \in [t_i, t_{i+1}],$$

where

$$w_i(t) = \frac{(t - t_{i+1})(t - t_{i+2})(t - t_{i+3})(t - t_{i+4})}{(t_i - t_{i+1})(t_i - t_{i+2})(t_i - t_{i+3})(t_i - t_{i+4})},$$
$$w_{i+1}(t) = \frac{(t - t_i)(t - t_{i+2})(t - t_{i+3})(t - t_{i+4})}{(t_{i+1} - t_i)(t_{i+1} - t_{i+2})(t_{i+1} - t_{i+3})(t_{i+1} - t_{i+4})},$$
$$w_{i+2}(t) = \frac{(t - t_i)(t - t_{i+1})(t - t_{i+3})(t - t_{i+4})}{(t_{i+2} - t_i)(t_{i+2} - t_{i+1})(t_{i+2} - t_{i+3})(t_{i+2} - t_{i+4})},$$
$$w_{i+3}(t) = \frac{(t - t_i)(t - t_{i+1})(t - t_{i+2})(t - t_{i+4})}{(t_{i+3} - t_i)(t_{i+3} - t_{i+1})(t_{i+3} - t_{i+2})(t_{i+3} - t_{i+4})},$$
$$w_{i+4}(t) = \frac{(t - t_i)(t - t_{i+1})(t - t_{i+2})(t - t_{i+3})}{(t_{i+4} - t_i)(t_{i+4} - t_{i+1})(t_{i+4} - t_{i+2})(t_{i+4} - t_{i+3})}.$$

The right splines we can use near the left boundary of the interval $[a, b]$ but not near the right boundary of the interval

$[a,b]$ as in the three grid intervals. The approximation with the left splines can be written as follows:

$$V_4^R(t) = \sum_{j=i-3}^{j=i+1} u(t_j) w_j(t),\ t \in [t_i, t_{i+1}],$$

where

$$w_{i-3}(t) = \frac{(t-t_{i-2})(t-t_{i-1})(t-t_i)(t-t_{i+1})}{(t_{i-3}-t_{i-2})(t_{i-3}-t_{i-1})(t_{i-3}-t_i)(t_{i-3}-t_{i+1})},$$

$$w_{i-2}(t) = \frac{(t-t_{i-3})(t-t_{i-1})(t-t_i)(t-t_{i+1})}{(t_{i-2}-t_{i-3})(t_{i-2}-t_{i-1})(t_{i-2}-t_i)(t_{i-2}-t_{i+1})},$$

$$w_{i-1}(t) = \frac{(t-t_{i-3})(t-t_{i-2})(t-t_i)(t-t_{i+1})}{(t_{i-1}-t_{i-3})(t_{i-1}-t_{i-2})(t_{i-1}-t_i)(t_{i-1}-t_{i+1})}$$

$$w_i(t) = \frac{(t-t_{i-3})(t-t_{i-2})(t-t_{i-1})(t-t_{i+1})}{(t_i-t_{i-3})(t_i-t_{i-2})(t_i-t_{i-1})(t_i-t_{i+1})},$$

$$w_{i+1}(t) = \frac{(t-t_{i-3})(t-t_{i-2})(t-t_{i-1})(t-t_i)}{(t_{i+1}-t_{i-3})(t_{i+1}-t_{i-2})(t_{i+1}-t_{i-1})(t_{i+1}-t_i)}$$

.

Theorem 2. The error of approximation with the middle polynomial splines of the fifth-order approximation when $t \in [t_j,\ t_{j+1}]$ is the following:

$$\|V_4^M - u\| \le K\ \|u^{(5)}\|_{[t_{i-2},t_{i+2}]} h^5/5!,\ K = 0.864.$$

The error of the approximation with the left polynomial splines of the fifth-order approximation is the following:

$$\|V_4^L - u\| \le K\ \|u^{(5)}\|_{[t_i,t_{i+4}]} h^5/5!, K = 3.632.$$

The error of the approximation with the right polynomial splines of the fifth-order approximation is the following:

$$\|V_4^R - u\| \le K\ h^5/5!\ \|u^{(5)}\|_{[t_{i-3},t_{i+1}]}, K = 3.632.$$

Proof. The proof of the theorem is based on the application of the Lagrangian interpolation remainder formula.

Table II shows the factual errors in absolute values of the approximation of function $u(x)$ when we use the left, the right, and middle splines of the fifth-order approximation when $[a,b] = [-1,1], h = 0.1$.

Table II. The factual errors of approximation with the left the right, and middle polynomial splines

Function $\boldsymbol{u(x)}$	The factual error of approximation		
	The Left splines	*The Right splines*	*The Middle splines*
$\frac{1}{1+25x^2}$	0.03372	0.03372	0.01244
$\sin(x)\cos(2x)$	0.00003625	0.00003625	0.00001414

Figs. 1-3 show the errors of approximation with the middle, the left and the right splines of the fifth-order approximation

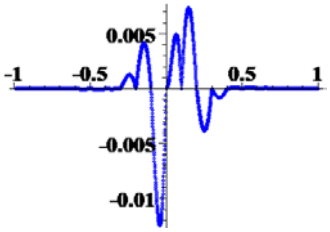

Fig.1 Plot of the error of approximation of $u = \frac{1}{1+25x^2}$ with the middle splines when $[a,b] = [-1,1],\ n = 20$

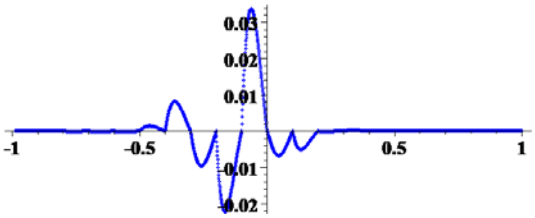

Fig.2 Plot of the error of approximation of $u = \frac{1}{1+25x^2}$ with the right splines when $[a,b] = [-1,1],\ n = 20$

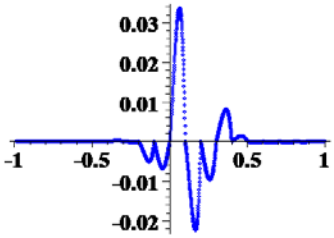

Fig.3 Plot of the error of approximation of $u = \frac{1}{1+25x^2}$ with the left splines when $[a,b] = [-1,1],\ n = 20$

C. Trigonometric splines of the third order of approximation

To apply an approximation using the left trigonometric splines, we construct an approximation in the form:

$$\tilde{u}^L(t) = u(t_j) w_j(t) + u(t_{j+1}) w_{j+1}(t) + u(t_{j+2}) w_{j+2}(t),$$
$$t \in [t_j, t_{j+1}],$$

where $w_j(t), w_{j+1}(t), w_{j+2}(t)$ we find by solving a system of equations:

$$\tilde{u}(t) = u(t), u(t) = \varphi_i, i = 1,2,3;$$

where

$$\varphi_1 = 1, \varphi_2 = \sin(t), \varphi_3 = \cos(t).$$

The solution of this system can be represented as follows:

$$w_j(t) = \frac{\sin(t/2 - t_{j+1}/2)}{\sin(t_j/2 - t_{j+1}/2)} \cdot \frac{\sin(t/2 - t_{j+2}/2)}{\sin(t_j/2 - t_{j+2}/2)},$$

$$w_{j+1}(t) = \frac{\sin(t/2 - t_j/2)}{\sin(t_{j+1}/2 - t_j/2)} \cdot \frac{\sin(t/2 - t_{j+2}/2)}{\sin(t_{j+1}/2 - t_{j+2}/2)},$$

$$w_{j+2}(t) = \frac{\sin(t/2 - t_j/2)}{\sin(t_{j+2}/2 - t_j/2)} \cdot \frac{\sin(t/2 - t_{j+1}/2)}{\sin(t_{j+2}/2 - t_{j+1}/2)}.$$

To apply an approximation using the right trigonometric splines, we construct an approximation in the form:

$$\tilde{u}^R(t) = u(t_{j-1})w_{j-1}(t) + u(t_j)w_j(t) + u(t_{j+1})w_{j+1}(t), \quad t \in [t_j, t_{j+1}].$$

The solution of this system can be represented as follows:

$$w_{j-1}(t) = \frac{\sin(t/2 - t_j/2)}{\sin(t_{j-1}/2 - t_j/2)} \cdot \frac{\sin(t/2 - t_{j+1}/2)}{\sin(t_{j-1}/2 - t_{j+1}/2)},$$

$$w_j(t) = \frac{\sin(t/2 - t_{j-1}/2)}{\sin(t_j/2 - t_{j-1}/2)} \cdot \frac{\sin(t/2 - t_{j+1}/2)}{\sin(t_j/2 - t_{j+1}/2)},$$

$$w_{j+1}(t) = \frac{\sin(t/2 - t_{j-1}/2)}{\sin(t_{j+1}/2 - t_{j-1}/2)} \cdot \frac{\sin(t/2 - t_j/2)}{\sin(t_{j+1}/2 - t_j/2)}$$

Theorem 3. Let function $u(x)$ be such that $u \in C^3[\alpha, \beta]$. Suppose $\{x_k\} \in [\alpha, \beta]$. is the set of nodes, such that $x_{j+1} - x_j = h$, $h < 1$. Then for $x \in [x_j, x_{j+1}]$ we have

$$|u(x) - \tilde{u}^R(x)| \le K_1 h^3 \parallel u''' + u' \parallel_{[x_j, x_{j+2}]},$$

$$|u(x) - \tilde{u}^L(x)| \le K_1 h^3 \parallel u''' + u' \parallel_{[x_{j-1}, x_{j+1}]},$$

where $K_i = 0.0835$.

Proof. Using representation (see [21])

$$u(x) = 2\int_{x_j}^{x} (u'''(x) + u'(x)) \sin^2 \frac{x-t}{2} dt + c_1 \sin(x) + c_2 \cos(x) + c_3,$$

(c_i are arbitrary constants) and the formulae for the left or right trigonometric splines we receive the estimation of the error of approximation.

Remark. Calculating the error of the approximation for function $u(x) = sin(x) - cos(x) + x$ we get the practical value which is very close to the theoretical value (see Tables III, IV). It can be calculated that for $u(x) = sin(x) - cos(x) + x$ we obtain $u''' + u' = 1$.

Table III shows the factual errors in absolute values of the approximation of function $u(x)$ when we use the left, or the right trigonometrical splines of the third -order approximation when $[a, b] = [-1,1], h = 0.1$. Table IV shows the theoretical errors in absolute values of the approximations with the trigonometric splines.

Table III. The factual errors of approximation with the left or the right trigonometric splines

Function $\boldsymbol{u(x)}$	The factual error of approximation	
	The Left splines	*The Right splines*
$\frac{1}{1+25x^2}$	0.0294	0.0294
$\sin(2x)\cos(x)$	0.000766	0.000766
$\sin(x)\cos(2x)$	0.000766	0.000766
$sin(x) - cos(x) + x$	0.000064	0.000064

Table IV. The theoretical errors of approximation with the left or the right trigonometric splines

Function $\boldsymbol{u(x)}$	The factual error of approximation	
	The Left splines	*The Right splines*
$\frac{1}{1+25x^2}$	0.0485	0.0485
$\sin(2x)\cos(x)$	0.001	0.001
$\sin(x)\cos(2x)$	0.001	0.001
$sin(x) - cos(x) + x$	0.0000835	0.0000835

III. ON REDUCING THE NUMBER OF INTERPOLATION NODES

Let us assume that the values of the function at the nodes are known. The approximation using the values of the function at the nodes of the grid and the basis splines of the third order of approximation is constructed. Is it possible to remove a certain number of nodes so that the approximation error changes slightly?

Using Theorems 1 and 2, it is possible to remove some nodes from the grid of the nodes, so that the approximation error is preserved on the new grid of nodes. For example. Let us take function $u(x) = \sin(x)\cos(2x)$. Let us take the interval $[a, b] = [-1,1], n = 20$ and equidistant set of nodes with $h = 2/n$. The plot of the error of the approximation is given in Fig. 4. The maximum in absolute value of the error of the approximation equal 0.000865.

If we take $n_1 = 10$ and construct the new equidistant set of nodes $x_{j+1} = a + jh$ with $h = 2/n_1$ we get the maximum in absolute value of the error of the approximation equal 0.0004373.

The plot of the error of the approximation is given in Fig. 5. It is easy to see that the nodes of the new grid are also included in the nodes of the previous grid of nodes.

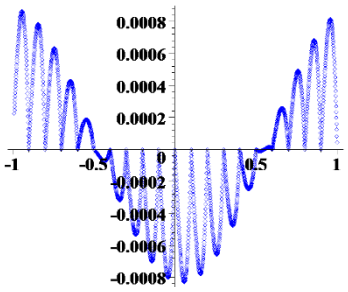

Fig.4 The error of approximation of the third order of function $u(x) = \sin(x)\cos(2x)$when $[a, b] = [-1,1],\ n = 20$

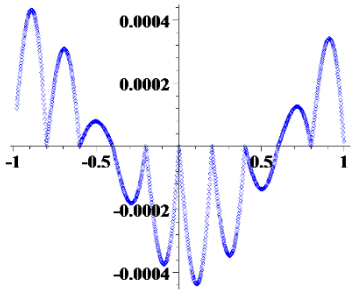

Fig.5 Plot of the error of approximation with splines of the fifth order of function $u(x) = \sin(x)\cos(2x)$ when $[a,b] = [-1,1],\ n_1 = 10$

IV. NUMERICAL ALGORITHM OF COMPRESSION THE FLOWS

Using the approximation error estimates, it is not difficult to suggest an algorithm for compressing and recovering numerical flows with the preservation of the approximation order.

A. Image Size Increasing Algorithm

Consider the case of increasing the image twice (in width and height) from 6x6 to 12x12. First, copy the source data to a sparse grid of nodes. In the case of increasing the size of the image exactly twice the problem arises, how to compare the original data with the new image. Let $i \in 1..M, j \in 1..N$, where M is the width, N is the height. If each pixel with coordinates (i,j) of the original image is associated with a pixel $(2*i-1,\ 2*j-1)$ from the enlarged image, then the added information about the colors will look like Fig.6:

Fig.6

But in this case we will not be able to calculate the color value in the last pixel. There are two solutions to this problem:

1). If a, b are the width and the height of the original image, x is an integer indicating how many times we want to enlarge the image, then we will take the dimensions of the new image equal: width $= (a-1) * x + 1$, height $= (b-1) * x + 1$. So the line we considered earlier will look like Fig.7:

Fig.7

and with the help of spline approximation we can calculate the values at intermediate points.

2) Increase the size by x times, but match the pixels as follows in Fig.8 (an example of increasing the size by 2 times):

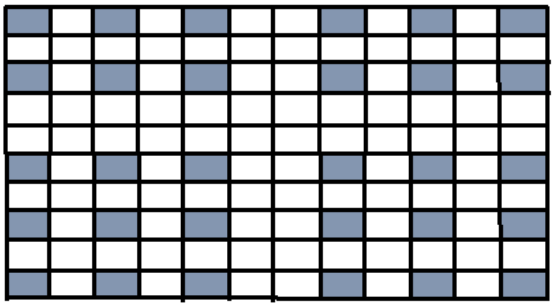

Fig.8

Next, for the left side, we look for an approximation with the right splines (green), for the right side with the left splines (red color) as it is shown in Fig.9

Fig.9

Then we repeat the procedure for the columns. For the upper part we are looking for an approximation with the right splines (green) and for the lower part - with the left splines (red). Thus, we calculate all the color values in the enlarged image (calculations are carried out for each color component: red, green, blue and α-channel).

The results of the enlarging of the images using the splines of the third order of approximation are presented in Figs. 10-12. Fig.10 shows the image of 150x150 pixels. Fig.11 shows the enlarged image of 300x300 pixels. Fig.12. shows the part of enlarged image of 600x600 pixels

Fig.10 The image of 150x150 pixels

If we compare the quality of images obtained with the different splines then we can notice the following: the results when we apply the polynomial splines or the trigonometric splines of the third order approximation are almost identical. In comparison with them, the images obtained using polynomial splines of the fifth order of approximation look smoother. The best is the picture obtained by approximation by polynomial splines of the fifth order of approximation. In Figure 13 it can be noticed the differences if you look at the eye area: on the bottom image, the combination of colors looks smoother. In addition, it is distinguished by a smaller amount of noise.

Fig.11 The enlarged image of 300x300 pixels

Fig.12 The enlarged image of 600x600 pixels

Fig.13 The image comparison

REFERENCES

[1] R. Abiantun, F. Juefei-Xu, U. Prabhu, M. Savvides, "Sparse signal recovery for single-image super-resolution on faces with extreme low resolutions," *Pattern Recognition*, vol. 90, pp. 308-324, 2010.

[2] B. Xue, S. Zheng, W. Xue, "Multi-scale adaptive factors video acceleration magnification," *Signal Processing: Image Communication*, vol. 71, pp.36-44, 2019.

[3] V. Diana Earshia, M. Sumathi, "A comprehensive study of 1D and 2D image interpolation techniques," *Lecture Notes in Electrical Engineering*, vol. 500, pp. 383-391, 2019.

[4] D. Abdullah, F. Fajriana, M. Maryana, L. Rosnita, A.P. Utama Siahaan, R.Rahim, P. Harliana, H. Harmayani, Z. Ginting, Erliana, D. Irwansyah Z. Zulmiardi, M. Khaddafi, F. Milanie, H. Aspan, I. Huda, K. Saddhono, I. Mulyaningsih, R.M. Moonti, P. Parwito, H. Djanggih, A. Amalia, E. Winarno, W. Hadikurniawati, "Application of Interpolation Image by using Bi-Cubic Algorithm," *Journal of Physics: Conference Series*, vol. 1114, no.1, 2018.

[5] Y. Wang, Q. Liu, H. Zhou, Y. Wang, "Learning multi-denoising autoencoding priors for image super-resolution," *Journal of Visual Communication and Image Representation*, vol. 57, pp.152-162, 2018.

[6] X. Wang, R. Song, A. Zhang, X. Ai, J. Tao, "Remote sensing image magnification study based on the adaptive mixture diffusion model," *Information Sciences*, vol. 467, pp. 619-633, 2018.

[7] H. Amri, M. Gargouri, M.K. Abdmouleh, A. Khalfallah, B. David, M. S. Bouhlel, "Discrete wavelet transforms for PET image reduction/expansion," *Advances in Intelligent Systems and Computing*, vol. 633, pp.524-539, 2018.

[8] P.Y. Chen, S.H. Lin, P.C. Chen, "Hardware implementation of an image interpolation method with controllable sharpness," *Journal of Information Science and Engineering*, vol. 34, no.1, pp. 51-64, 2018.

[9] C. Luckner, T. Mertelmeier, A. Maier, L. Ritschl, "Towards full-body X-ray images," *Informatik aktuell*, pp. 86-91, 2018.

[10] Q. Cao, A. Sisniega, M. Brehler, J.W. Stayman, J. Yorkston, J. H. Siewerdsen, W. Zbijewski, "Modeling and evaluation of a high-resolution CMOS detector for cone-beam CT of the extremities," *Medical Physics*, vol. 45, no.1, pp.114-130, 2018.

[11] R. Dahl, M. Norouzi, J. Shlens, "Pixel Recursive Super Resolution," *in Proceedings of the IEEE International Conference on Computer Vision*, pp.5449-5458, 2017.

[12] N.E. Farthing, R.C. Findlay, J.F. Jikeli, P.B. Walrad, M.A. Bees, L.G. Wilson, "Simultaneous two-color imaging in digital holographic microscopy," *Optics Express*, vol. 25, no. 23, pp.28489-28500, 2017.

[13] Y. Men, G. Zhang, C. Men, X. Li, N. Ma, "A sub-pixel disparity refinement algorithm based on Lagrange interpolation," *Chinese Journal of Electronics*, vol. 26, no. 4, pp.784-789, 2017.

[14] A. Sarno, D.R. Dance, R.E. Van Engen, K.C. Young, P. Russo, F.Di Lillo, G. Mettivier, K. Bliznakova, B. Fei, I. Sechopoulos, "A Monte

Carlo model for mean glandular dose evaluation in spot compression mammography," *Medical Physics*, vol. 44, no. 7, pp.3848-3860, 2017.

[15] G. Rosline, N. Kumari, M. Yuvaraju, "High quality image scaling using interpolation techniques with filters," *International Journal of Pharmacy and Technology*, vol. 8, no. 4, pp.19863-19873, 2016.

[16] G. Sreedevi, P.K. Narayanamurthy, C.S. Seelamantula, "Efficient resampling of speech/audio signals in shift-invariant spaces," *22nd National Conference on Communication*, NCC, no. 7561145, 2016.

[17] V. Skala, M. Smolik, "A new approach to vector field interpolation, classification and robust critical points detection using radial basis functions," *Advances in Intelligent Systems and Computing*, no. 765, pp. 109-115, 2019.

[18] Yu.K. Dem'yanovich, "General flows and their adaptive decompositions," *Wseas Transactions on Mathematics*, vol. 17, pp.28-34, 2018.

[19] I. G. Burova, V. M. Ryabov, M. A. Kalnitskaia, A. V. Malevich, "The Interpolation Method for Calculating Eigenvalues of Matrices," *WSEAS Transactions on Systems and Control*, vol. 14, pp. 104-111, 2019.

[20] I.G. Burova, O.V. Rodnikova, "Integro-differential polynomial and trigonometrical splines and quadrature formulae," *WSEAS Transactions on Mathematics*, vol.16, pp. 11-18, 2017.

[21] I.G. Burova, "On left integro-differential splines and Cauchy problem," International Journal of Mathematical Models and Methods in Applied Sciences, vol. 9, pp. 683-690, 2015.